

CAPILLARY DRIVEN FUEL SUPPLY IN DIRECT METHANOL FUEL CELLS WITH DOUBLE TAPERED T-SHAPED CHANNEL FLOW FIELDS

N. Paust, C. Litterst, T. Metz, M. Eck, R. Zengerle and P. Koltay

Laboratory for MEMS Applications, Department of Microsystems Engineering (IMTEK), University Freiburg, Georges-Köhler-Allee 106, D-79110 Freiburg, Germany

ABSTRACT

This paper presents a new concept for passive degassing and fuel supply in Direct Methanol Fuel Cells (DMFCs). The potential energy of deformed CO₂ bubbles, generated as a reaction product during DMFC operation, is employed to propel the fluidic flow. In our previous work [1], we have shown that passive degassing can be achieved by capillary forces. The present work combines passive degassing with capillary driven fuel supply. In contrast to a passive valve based approach presented by Meng and Kim [2], we discuss and evaluate the performance of double tapered T-shaped channels to achieve fully autonomous DMFC operation. A proof of principle is performed applying CFD-simulations. Bubble configurations and the pumping performance of double tapered T-shaped channels are studied experimentally for different channel surface conditions under various gas flow rates. Applying these channels, the fully passive operation of a DMFC for more than 12 hours could be demonstrated.

1. INTRODUCTION

It is a well known phenomenon that gas bubbles in micro fluidic systems can cause high pressure losses or even complete channel blocking [3]. A unique solution to prevent such clogging has been presented by Kohnle et al. [4] applying T-shaped channels. Fig. 1 shows a cross section of a T-shaped channel with three different bubble configurations. Depending on geometric parameters, gas bubbles can block the T-channel (Fig. 1a), fill the root (Fig. 1b), or fill the branch of the T (Fig. 1c) only. Compared to rectangular channels, the configuration b and c increase the mobility of gas bubbles due the unblocked liquid bypasses as further detailed in [4]. In our previous work [1], a double tapered T-shaped channel as depicted in Fig. 3 has been applied to safely remove carbon dioxide bubbles that are generated as a reaction product on the anode of a DMFC:



The bubble removal is exclusively propelled by capillary forces. In the present work, the design of the DMFC system with the T-shaped anode channels has been modified so that the moving CO₂ bubbles additionally pump the fuel. On the

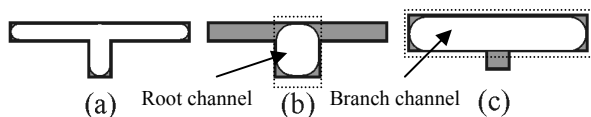


Fig. 1: Cross section of possible bubble shapes (white) in T-shaped channels.

cathode, oxygen is supplied by diffusion and natural convection [5]. Therefore, the DMFC operates fully passive with no need of any external actuation.

2. WORKING PRINCIPLE

A schematic time sequence of a growing bubble above an inlet in a tapered channel is depicted in Fig. 2. As the pressure in the gas inlet exceeds the capillary pressure:

$$\Delta p = \sigma \kappa \quad (2)$$

(σ represents surface tension and κ the curvature of the liquid gas interface) of the liquid gas interface of a half sphere above the inlet, a bubble is formed. As the bubble grows, it touches the upper channel wall at some point ($t = t_1$) and becomes continuously deformed developing interfaces with increasingly different curvatures at the front and the back of the bubble ($t = t_2$). These different curvatures result in a pressure difference over the whole bubble that induces a flow that

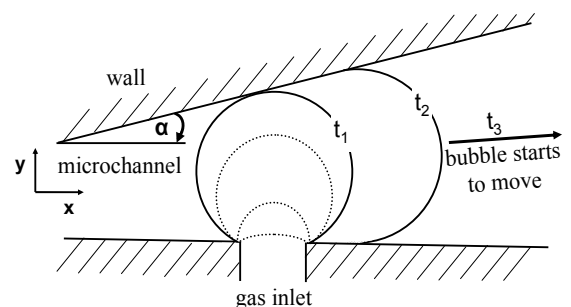


Fig. 2: Schematic time sequence of a growing gas bubble in a tapered channel.

transports the bubble towards the opening of the tapered channel. However, before starting to move, contact line pinning keeps the bubble in place [6]. The bubble continues growing until the pinning force is overcome ($t = t_3$). Subsequently, the bubble detaches from the inlet and moves towards the opening of the channel. This process also takes place in a tapered T-shape channel as depicted in Fig. 3, if the bubble is positioned in the root of the channel as shown in Fig. 1(b).

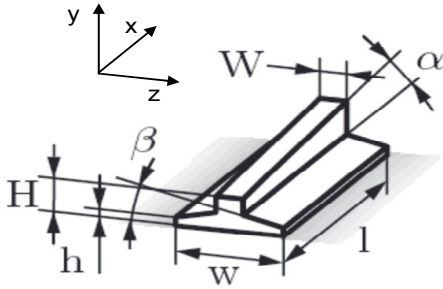


Fig. 3: Investigated double tapered T-shaped channel structure. $W = 800 \mu\text{m}$, $w = 3000 \mu\text{m}$, $H = 800 \mu\text{m}$, $h = 300 \mu\text{m}$, $l = 20000 \mu\text{m}$, $\alpha = 3^\circ$, $\beta = 7^\circ$.

Fig. 3 shows the channel geometry that has been investigated in the present work. It contains sections which are tapered by a tapering angle β (“branch channel”). The tapering of the branch channel causes gas bubbles to move in the “root channel” in the middle of the structure. Subsequently, the tapering of the root channel (tapering angle α) transports the bubble to the channel end. To ensure the proper functioning of this mechanism, the bubbles must adopt the position (b) in Fig. 1. That this is indeed the case can be assured by the dimensioning of the root and the branch channel as further detailed in [7]. Whether a bubble indeed moves from the branch channels into the root channel is a matter of size. Especially the dynamics of moving contact lines, and the effect of contact line pinning [6] play a key role. As mentioned earlier in context with Fig. 2, in tapered channels the gas bubbles must exceed a certain size before starting to move. Therefore, small bubbles can block the branch channels. In this situation, liquid displaced by a “large” bubble moving along the root channel can not completely recirculate through the branch channel, which is most of the time partly obstructed by “small” bubbles. Thus, a considerable amount of the displaced liquid is

directed towards the channel end and can be piped through an outer loop, such that liquid is effectively pumped.

In the following, the ratio of the liquid flow rate induced by the growing and moving bubbles compared to the gas flow rate will be referred to as the pumping efficiency (p_{eff}). According to Eq. 3, the molar flow of produced CO_2 is equal to the molar flow of methanol consumed. Thus, the minimum required pump efficiency to sustain the operation of a DMFC yields:

$$p_{eff} = \frac{\rho_{\text{CO}_2}}{M_{\text{CO}_2} C_f} \quad (3)$$

where M_{CO_2} is the molecular weight of CO_2 , C_f is the molar concentration of the water-methanol solution and ρ_{CO_2} is the density of carbon dioxide. In the present work, a methanol concentration of the water methanol solution of 4 mol L^{-1} has been investigated. The minimum required pump efficiency is therefore $p_{eff} = 1\%$. In other words: The required methanol supply rate is only about 1% of the generated CO_2 flow rate. In the following, it will be shown that this minimum pump efficiency can be achieved by the investigated channel structure.

3. PROOF OF PRINCIPLE

Prior to the experimental study, a proof of principle has been performed with computational fluid dynamic (CFD) simulations applying the commercial software CFD-ACE+ from ESI-Group [8]. Fig. 4 (top) shows a time sequence of moving CO_2 bubbles in the double tapered T-shaped channel structure. Standard methods have been applied to track the free interfaces with a static contact angle taken from measurements of a 4 M water methanol solution on PMMA ($\theta \approx 35^\circ$). With respect to symmetry, only half of the channel was simulated. The bubbles are generated using mass source terms at six different places evenly distributed over the bottom of the simulated geometry. From Fig. 4 (top), it can be seen that the growing bubbles in the branch channels remain stationary until they reach a certain size and move into the root channel. Here, bubbles merge and form big bubbles that move towards the opening of the root channel and thereby pump the fuel ($p_{eff} = 0.28$ at $\Phi_{\text{gas}} = 320 \mu\text{L}$).

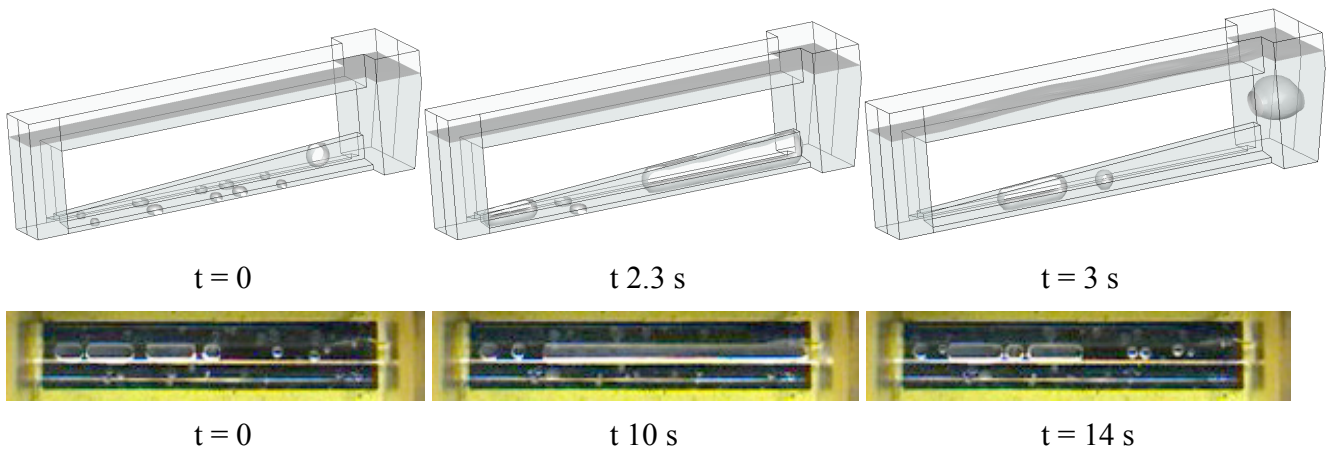


Fig. 4: Time sequence of growing and moving bubbles in double tapered T-shaped channels ($\alpha = 3^\circ$, $\beta = 7^\circ$) during DMFC operation. Top: CFD simulation ($\Phi_{\text{gas}} = 320 \mu\text{L min}^{-1}$) Bottom: Fuel cell experiments. $\Phi_{\text{gas}} \approx 51 \mu\text{L min}^{-1}$.

Fig. 4 (top) exhibits a good qualitative agreement with experimental results depicted in Fig. 4 (bottom). However, the computational effort was very demanding (about two weeks on a single processor AMD Opteron 2.0 GHz) for the time sequence of Fig. 4 (top) and the applied static contact angle model was not fully validated, especially for the porous gas diffusion layer covering the channel bottom in the anode flow field of the DMFC. Therefore, the pumping performance has been studied experimentally.

4. EXPERIMENTAL RESULTS

The pumping efficiency has been investigated with an experimental set-up as depicted in Fig. 5. In this configuration, the gas flow was supplied by three syringe pumps. In Fig. 6, the pump efficiency – which was calculated from the applied gas flow rate and the measured liquid flow rate – is plotted against the total gas flow rate for different surface properties. For the hydrophilic configuration, the channel walls have been coated with a silicate oxygen layer in order to obtain complete wetting. The contact angle is close to zero, thus, the three phase contact line almost vanishes and contact line pinning plays a minor role. Growing bubbles in the side channels move into the center channel as soon as they become deformed by the channel walls. Therefore, the branch channels are never blocked and the major part of the displaced liquid recirculates around the large bubble in the

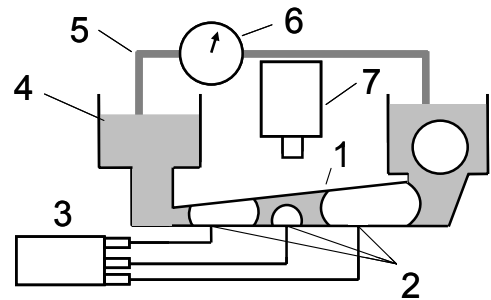


Fig. 5: Experimental set-up for the investigation of pumping efficiencies in double tapered T-shaped structures. (1): Double tapered T-shaped channel (Fig. 3), (2): Six gas inlets evenly distributed at the channel bottom supplied by a syringe pump (3) (Braun Melsungen), (4): Reservoir, (5): Tube, (6): Flow sensor (Sensirion) (7): Camera (Phillips webcam).

root channel not contributing to the pumping mechanism. The overall pump efficiency is very small ($p_{\text{eff}} \approx 0.1\%$). The more realistic case for DMFC operation is the untreated channel (black line in Fig. 6) with the channel bottom covered by a gas diffusion layer (SGL, [®]SIGRACET GDL31-BA). In this configuration, the porous rough surface of the carbon fibers causes severe pinning. Gas bubbles in the side channels block the recirculation path and a significant amount of the displaced liquid is effectively pumped. The pump efficiency is almost two orders of magnitude higher than in the hydrophilic case with a maximum value of $p_{\text{eff}} \approx 10\%$ at a gas flow rate of $\Phi_{\text{gas}} = 185 \mu\text{L min}^{-1}$.

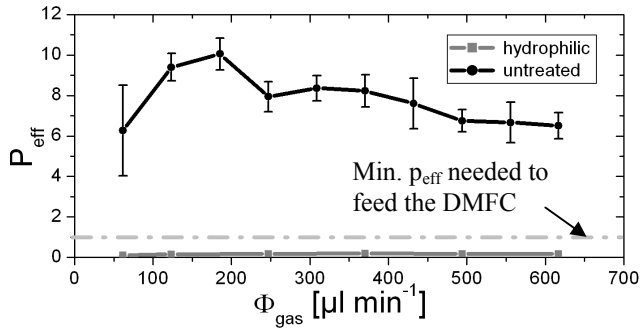


Fig. 6: Pumping performance of double tapered T-shaped channels at various gas flow rates.

Finally, the channel geometry as depicted in Fig. 3 has been applied to realize a fully autonomous operating DMFC. The anode flow field was realized by three parallel untreated channels as discussed before. Fig. 4 (bottom) shows a time sequence of a top view on one channel of the anode flow field during DMFC operation. Large CO₂ bubbles merge in the center channel while small bubbles remain in the side channel due to the previously discussed pinning effect. As in the experiments with syringe pump driven gas flow, small bubbles do block the branch channels ensuring that the moving bubbles in the root channel effectively transport liquid to sustain the operation of the DMFC. Long term experiments were performed at the maximum power output of the DMFC at a constant current of 20 mA cm⁻² corresponding to a theoretical gas flow rate of 50 μL min⁻¹. In Fig. 7, the power output of the DMFC is plotted against time. A continuous operation with a power output of about 6 mW for more than 12 hours could be observed before the operation stopped due to fuel depletion and starving.

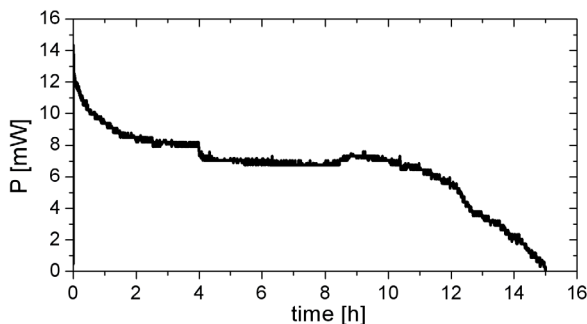


Fig. 7: Power performance of long term measurements of a fully passive DMFC with an anode flow field consisting of 3 parallel double tapered T-shaped channels. Active MEA area (Umicore): $A_{MEA} = 3 \text{ cm}^2$.

5. CONCLUSIONS

A novel anode flow field geometry for the fully passive operation of a DMFC has been presented. A proof of principle of the capillary supply system has been performed with CFD simulation. The pumping mechanism was investigated with experiments showing that a maximum pump efficiency of $p_{eff} \approx 10\%$ can be achieved with the presented structure. Finally, the flow field has been proofed to sustain the fully passive operation of a DMFC until the fuel of the reservoir was consumed completely.

ACKNOWLEDGEMENTS

This work was supported by the German Ministry of Science and Education within Project 03SF0311B, the German Federal Ministry of Economics and Labour (BMWA) within the VDI/VDE InnoNet-program PlanarFC and the German Research Council within Project 527/3.

REFERENCES

- [1] C. Litterst, S. Eccarius.; C. Hebling; R. Zengerle; P. Koltay, *Journal of Micromechanics and Microengineering*, Vol. 16, No. 9, pp. 248-253, 2006.
- [2] D. D. Meng and C.-J. Kim, *Proceedings of IEEE MEMS*, Kobe 2007, pp. 85-88.
- [3] P. Gravesen, J. Braneberg; O.S. Jensen, *Journal of Micromechanics and Microengineering*, Vol. 3, No. 4, pp. 168-182, 1993.
- [4] J. Kohnle, G. Waibel, R. Cernosa, M. Storz, H. Ernst, H. Sandmaier, T. Strobelt and R. Zengerle, *Proceedings of IEEE MEMS*, Las Vegas 2002, pp. 77-80.
- [5] C.Y. Chen; P. Yang, *Journal of Power Sources*, Vol. 123, No. 1, pp. 37-42, 2003.
- [6] L.C. Gao; T.J. McCarthy, *Langmuir*, Vol. 22, No. 14, pp. 6234-6237, 2006.
- [7] C. Litterst; J. Kohnle; H. Ernst; S. Messner; H. Sandmaier; R. Zengerle.; P. Koltay. *ACTUATOR. H. Borgmann*, Ed. Bremen: 2004, pp. 541-544.
- [8] www.esi-group.com